ISBN 978-90-481-2890-7

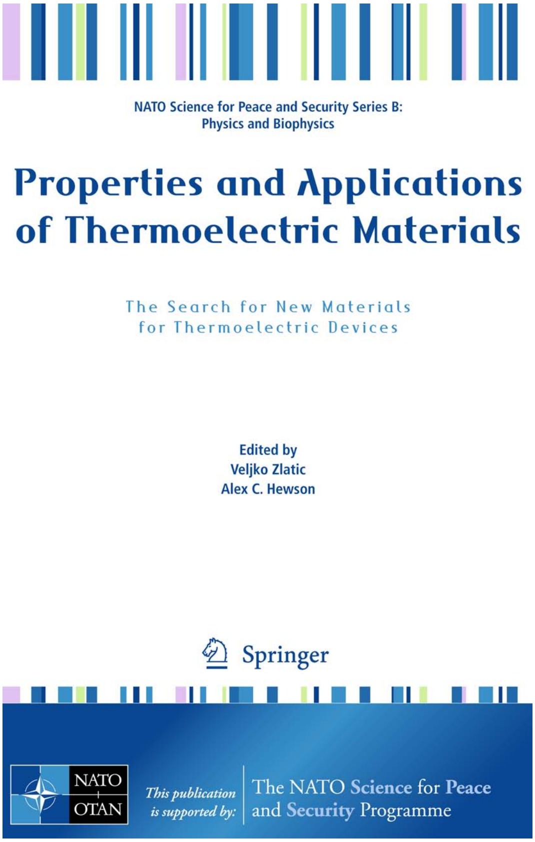

NATO Science for Peace and Security Series B:
Physics and Biophysics

Properties and Applications of Thermoelectric Materials

The Search for New Materials
for Thermoelectric Devices

Edited by
Veljko Zlatic
Alex C. Hewson

Springer

NATO OTAN
This publication is supported by: The NATO Science for Peace and Security Programme

New Approaches to Thermoelectric Materials

A. P. Gonçalves, E. B. Lopes, E. Alves, N. P. Barradas, N. Franco, O. Rouleau, and C. Godart

Abstract A deeper understanding of the parameters that affect the dimensionless figure of merit, the development of new concepts and the use of innovative synthesis techniques has recently led to systems with better thermoelectric performances. Here we present part of the work that has been recently performed in our groups in order to get new and improved thermoelectric systems. Two new systems, electrical conducting glasses and doped tellurium films, are proposed as new families of thermoelectric materials.

Abbreviations

S	Seebeck coefficient
V	Electrical potential
T	Absolute temperature
I	Electrical current
Q	Heat quantity
Π	Peltier coefficient
τ	Thomson coefficient
ZT	Figure of merit
σ	Electrical conductivity
λ	Thermal conductivity

A. P. Gonçalves and E. B. Lopes
Dep. Química, Instituto Tecnológico e Nuclear/CFMC-UL, P-2686-953 Sacavém, Portugal
e-mail: apg@itn.pt, eblopes@itn.pt

E. Alves, N. P. Barradas, and N. Franco
Dep. Física, Instituto Tecnológico e Nuclear/CFN-UL, P-2686-953 Sacavém, Portugal
e-mail: ealves@itn.pt, nunoni@itn.pt, nfranco@itn.pt

O. Rouleau and C. Godart
CNRS, ICMPE, CMTR, 2/8 rue Henri Dunant, 94320 Thiais, France
e-mail: rouleau@icmpe.cnrs.fr, godart@icmpe.cnrs.fr

V. Zlatić and A. C. Hewson (eds.), *Properties and Applications of Thermoelectric Materials*,
NATO Science for Peace and Security Series B: Physics and Biophysics,

$S^2\sigma$	Power factor
λ_e	Electronic contribution to the thermal conductivity
λ_L	Lattice (phonon) contribution to the thermal conductivity
PGEC	Phonon Glass Electron Crystal
T_g	Glass temperature
T_C	Crystallization temperature
ρ	Electrical resistivity
GIXRD	Grazing incidence x-ray diffraction
SEM	Scanning electron microscopy
EDS	Energy dispersive x-ray spectroscopy
RBS	Rutherford backscattering spectroscopy
ρ_{Bi}	Electrical resistivity of bismuth doped tellurium regions

1 Introduction

The climate changes that are being observed on a planetary scale, together with the recent oil crisis, has woken up public opinion to the serious consequences of an exaggerated consumption of primary resources and increase of pollution. A better use of energy became top priority for most of the developed countries, in particular of the European Union.

Following its general environmental politics, which has as primary objective to keep the maximum increase of the average world temperature below 2°C, the European Union has recently established as main targets a 20% decrease of greenhouse effect gases emission (when compared with the 1990 levels), a 20% increase of the energy efficiency and a rise of the renewable energy sources proportion to 20% by 2020.

The research of new environment friendly energy sources and the energy consumption optimization are therefore priority targets. A huge and almost unexplored reservoir of "green" energy is the electricity generation from temperature gradients. Thermoelectric materials are able to convert directly electrical energy into thermal energy and, reversibly, thermal energy into electrical. In many applications, thermoelectric energy generation uses zero-cost input energy (waste, heat of exhaust pipe of cars, etc.). Moreover, the complete absence of moving parts and the absence of substances as fluorinated cooling agents makes thermoelectric devices highly attractive.

The actual thermoelectrical devices use materials developed until the early 1960s, mainly based on the Bi_2Te_3 and Si–Ge phases. However, their efficiency is small ($<10\%$). It is therefore fundamental to identify new systems which could lead to higher device efficiencies.

A deeper understanding of the parameters that affect the thermoelectric performance, the development of new concepts and the use of innovative synthesis techniques have recently led to the identification of materials, as skutterudites, clathrates, half-Heusler and low dimensional systems, with improved thermoelectric characteristics (see review by Godart et al. in this volume [1]). However, the efficiency increase is limited in bulk materials and the cost of low dimensional systems is very high and therefore new systems need to be identified. In the next section the fundamentals of the thermoelectric effects and figure of merit will be presented, together with the new concepts on the parameters that affect the thermoelectric performance. Section 3 is devoted to the presentation of two new systems with promising thermoelectric performances. Finally, this chapter will finish with a conclusions section.

2 The Thermoelectric Effects and Figure of Merit

The three thermoelectric effects, Seebeck, Peltier and Thomson, were discovered during the first half of the nineteenth century. The first one was discovered by Seebeck, in 1821, and consists in the formation of an electrical potential difference, ΔV, when a circuit made of two different electrical conducting materials is submitted to a temperature gradient, ΔT. The Seebeck coefficient is defined as $\mathbf{S} = \Delta\mathbf{V}/\Delta\mathbf{T}$.

Peltier effect was discovered in 1834: when an electrical current, I, is applied to the circuit there is a heat absorption, Q, in one of the junctions and its liberation on the other. The Peltier coefficient is given by $\Pi = \mathbf{Q}/\mathbf{I}$.

The third thermoelectric effect, the Thomson effect, is observed when there are simultaneously present in an electrical circuit, a temperature gradient and an electrical current. There is absorption or liberation of heat in each individual segment of the circuit, being the thermal flux given by $\mathbf{dQ/dx} = \tau\mathbf{I}\ \mathbf{dT/dx}$, where $\mathbf{x}$ represents the spatial coordinate and τ is the Thomson coefficient of the material. Thomson also show that the Seebeck and Peltier effects are related by $\Pi = \mathbf{S}.\mathbf{T} = \mathbf{Q}/\mathbf{I}$.

The optimization of a compound or material for thermoelectrical applications mainly implies the maximization of a dimensionless number, the figure of merit ZT, that depends only on the material and is given by

$$\boldsymbol{ZT} = \mathbf{S}^2\mathbf{T}\sigma/\lambda,$$

where $\mathbf{T}$ represents the absolute temperature, $\mathbf{S}$ is the Seebeck coefficient, and σ and λ represent the electrical and thermal conductivities, respectively (for a deeper examination of the efficiencies of a thermoelectric material see review by Godart et al. in this volume [1]). ZT maximization can be done via both the maximization of the numerator, $\mathbf{S}^2\sigma$ (also called power factor), and the minimization of the denominator (thermal conductivity).

Figure 1 shows the Seebeck coefficient, electrical conductivity and power factor as a function of the charge carriers concentration on a logarithmic scale. The Seebeck coefficient decreases with the increasing concentration, whereas the electrical conductivity increases. Therefore, a maximum on the power factor is observed for concentrations of $\sim 10^{18}$–10^{21} carriers/cm^3, which correspond to low gap semiconductors or semimetals. The identification of Bi_2Te_3-based materials, which

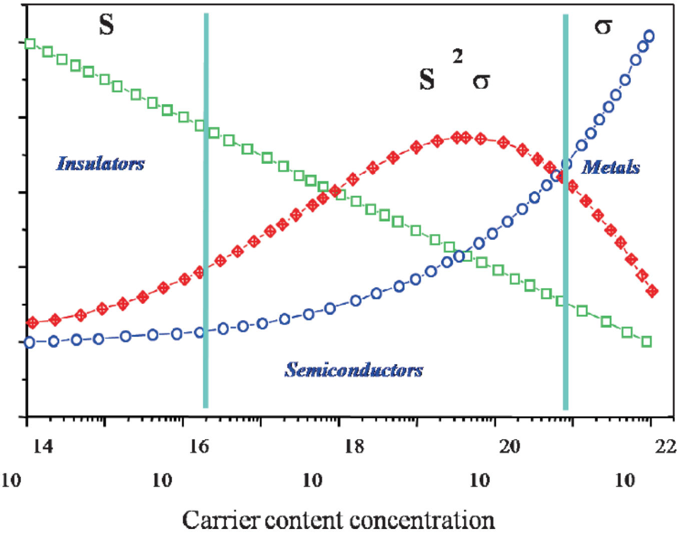

Fig. 1 Maximization of the power factor, $\mathbf{S}^2\sigma$, through carrier concentration tuning.

have $ZT \sim 1$ and are one of the most used materials for commercial thermoelectrical devices, followed this criterion.

The thermal conductivity is a second factor that must be optimized in order to maximize ZT: a material will increase its thermoelectric performance with the decrease of its thermal conductivity.

The thermal conductivity can be seen as a sum of two main different contributions, $\lambda = \lambda_\mathrm{e} + \lambda_\mathrm{L}$, where λ_e represents the electronic contribution and λ_L is the contribution from the lattice vibrations (phonons). The electronic contribution to thermal conductivity is related with the electrical conductivity via the Wiedemann–Franz law, $\lambda_\mathrm{e} = \mathbf{LT}\sigma$, where $\mathbf{L}$ represents the Lorentz factor. Therefore, ZT can be rewritten as

$$ZT = \frac{S^2}{L} \frac{\lambda_e}{\lambda_e + \lambda_L}$$

being evident that its maximization implies the minimization of the phonons contribution.

At the beginning of the 1990s Slack presented the new concept of “Phonon Glass Electron Crystal” (PGEC) [2], which proposes the research of compounds that conduct the electricity as a crystalline material and the heat as a glass. Based on this concept new improved thermoelectric materials, as skutterudites and clathrates, have been identified. The research of new thermoelectric systems based on the PGEC concept has lead to an intense effort to understand better the mechanisms that affect the phonons propagation without changing significantly the electrical charge propagation. Some general rules have been identified from these works, the most important ones being presented in Table 1. It must be stressed that these rules are not exclusive and several can exist simultaneously in the same material.

Table 1 Main general approaches to develop improved thermoelectrical systems by using the "Phonon Glass Electron Crystal" concept.

Approach	Effects on phonons	Materials (examples)
Heavy atoms weakly bounded to the structures	Phonon-scattering centers	Skutterudites, clathrates
Complex structures	Increase the optical phonon modes	Clathrates, $Yb_{14}MnSb_{11}$
Inclusions, impurities	Increase diffusion (affects more phonons than carriers)	Composites
Solid solutions	Increase mass fluctuations (higher phonon scattering)	Half-Heusler systems
Grain boundaries	Reduce the phonons mean free path	Low dimensional systems

3 New Systems

3.1 Conducting Glasses

A careful analysis of the main general approaches recently developed to obtain improved thermoelectric systems shows that the new materials must have complex structures, including the presence of inclusions and impurities, and should have mass fluctuations and disorder. A type of materials that follows all these principles are the glasses. Indeed, they have extremely complex structures, with a certain degree of order only at small distances, and present mass fluctuations, easily allowing high concentrations of inclusions and impurities.

Metallic glasses have been widely studied in the 1970s–1980s. The reported electrical conductivity and Seebeck coefficient values indicate that these types of materials are not suitable for thermoelectrical applications: in fact, they show Seebeck coefficients values typical of metals, ranging between $\pm 5\ \mu V/K$ [3–7]. Moreover, their electrical conductivity is smaller than the crystalline counterparts due to the intrinsic disorder. However, it is known that the maximum of the power factor is observed for low gap semiconductors and semimetals, and not for metals. Therefore, to identify glasses with improved thermoelectric performances it is necessary to center the investigation on the low gap semiconductor and semimetal glasses.

Numerous semiconducting glasses have been reported in the literature (see, for instance, [8, 9]), most of them based on pnictides and chalcogenides. One in particular, $Ge_{20}Te_{80}$, is based only on two elements, is formed mainly by heavy atoms, and has been described as easy to prepare [10]. Moreover, its electrical transport properties have already been studied, being reported as having high Seebeck coefficients, albeit presenting small electrical conductivity values [11]. Previous works have also shown that doping it with copper or silver can increase dramatically the

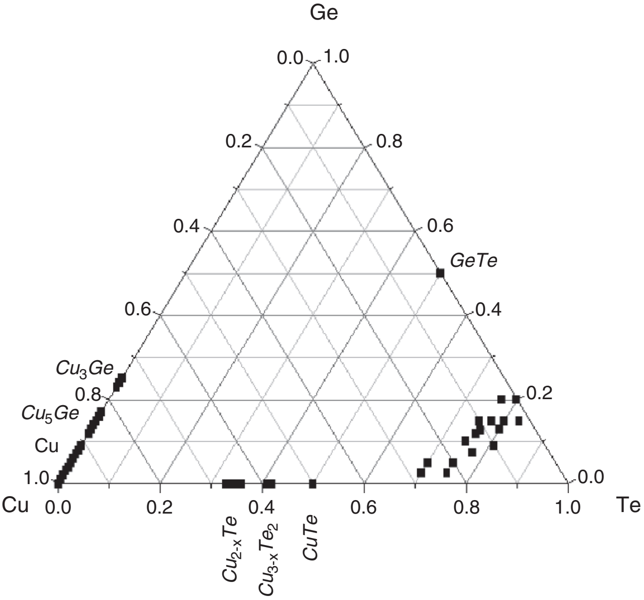

Fig. 2 $Cu_xGe_yTe_z$ general composition glasses (*black squares*) studied in the work presented in [14].

electrical conductivity [12,13]. For all these reasons we decided to use the $Ge_{20}Te_{80}$ glass as a starting test material, in order to check the possibility of optimizing the thermoelectrical performance of a glass by changing its composition [14].

Several samples with $Cu_xGe_yTe_z$ general compositions close to $Ge_{20-x}Te_{80-y}Cu_{x+y}$ (Fig. 2), together with the $Cu_{25}T_5Te_{70}$ ($T = Si$, Ga) ones, have been prepared by melt spinning, as described elsewhere [14]. The quality of the samples was checked by powder x-ray diffraction and differential thermal analysis measurements, together with optical microscope observations.

The materials have in general a glassy aspect (Fig. 3a), the disordered state being confirmed by the x-ray diffraction results for most of the samples (Fig. 4) [14]. However, it has been observed that some materials with higher copper concentrations frequently present regions where crystallization already starts (Fig. 3b), most probably being a sign of inhomogeneities on the cooling. X-ray diffractograms, made on powders representative of the totality of the sample, also reflect this reality, many of the higher copper concentration samples showing small crystallization peaks. The extreme composition $Cu_{30}Te_{70}$, albeit still presenting some disorder, is already crystallized and its electrical transport properties were not studied. The higher facility for samples with larger copper concentration to crystallize can be also deduced from the differential thermal analysis measurements: a decrease of the glass and crystallization temperatures are observed for the doped materials, when compared with the $Ge_{20}Te_{80}$ (Fig. 5). Therefore, it can be concluded that there is a decrease of the glass stability with the increase of the copper concentration, which implies higher

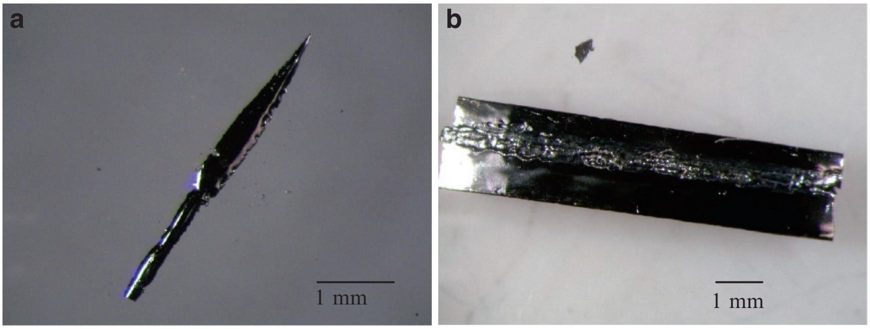

Fig. 3 Optical micrographs of the $Cu_{15}Ge_{7.5}Te_{77.5}$ (**a**) and $Cu_{22.5}Ge_{2.5}Te_{75}$ (**b**) melt-spinning samples.

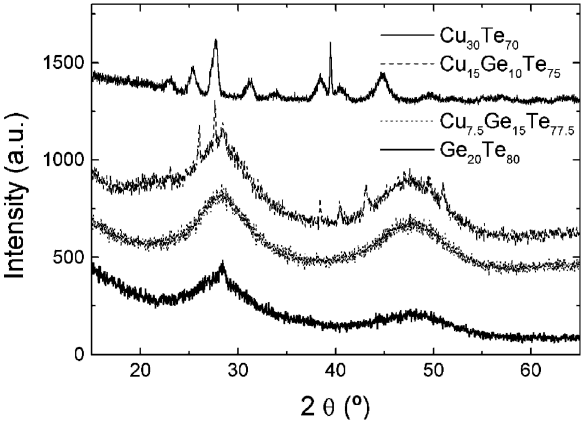

Fig. 4 Powder x-ray diffractograms of the $Ge_{20}Te_{80}$, $Cu_{7.5}Ge_{15}Te_{77.5}$, $Cu_{15}Ge_{10}Te_{75}$ and $Cu_{30}Te_{70}$samples.

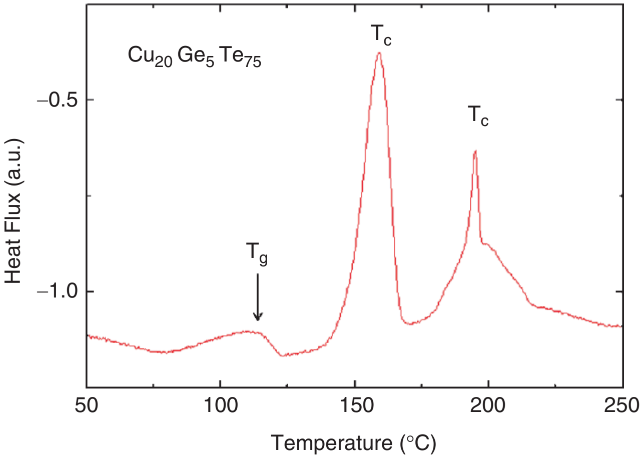

Fig. 5 Differential scanning calorimetric thermogram of the $Cu_{20}Ge_5Te_{74}$ glass sample. T_g and T_C represent, respectively, the glass and crystallization temperatures.

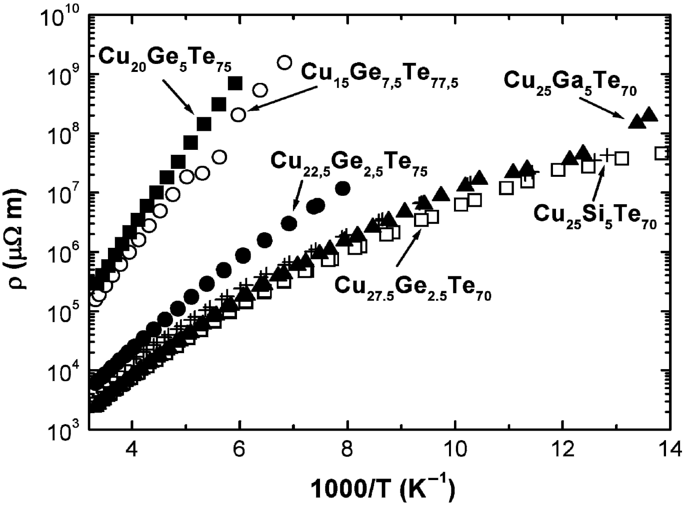

Fig. 6 Temperature dependence of the electrical resistivity for the $Ge_{20}Te_{80}$-based glasses.

cooling rates to obtain the disordered state. Moreover, the low glass transition temperature limits their use to temperatures close to the ambient. For all these reasons, the study of the effect of glass stabilizers addition on $Ge_{20}Te_{80}$-based glasses needs to be performed.

The thermoelectric performance of $Ge_{20}Te_{80}$-based conducting glasses was tested by measuring their Seebeck coefficients and electrical resistivities as a function of the temperature [14]. Special care was taken in order to make the measurements on purely glassy pieces, preferably with a needle-like shape.

All samples show a semiconductor behavior, with the electrical resistivity increasing with the decreasing temperature (Fig. 6). A strong dependence of the resistivity with the composition is observed. The analysis of the influence of the different components concentration in the electrical resistivity (Table 2) indicates that copper concentration is the main factor: a decrease on the room temperature electrical resistivity of five orders of magnitude can be observed when the composition changes from $Ge_{20}Te_{80}$ ($\sim 3\times 10^8$ μΩ m [11]) to $Cu_{27.5}Ge_{2.5}Te_{70}$ ($\sim 3\times 10^3$ μΩ m) [14]. Moreover, a decrease of the energy gap from ~0.47 to ~0.13 eV is also observed when changing from $Ge_{20}Te_{80}$ to $Cu_{27.5}Ge_{2.5}Te_{70}$ [11, 14].

Given the strong dependence of the electrical conductivity with composition one could also expect a corresponding huge change of the Seebeck coefficient. However, only a decrease from 960 μV/K to 394 mV/K has been observed for the extreme compositions ($Ge_{20}Te_{80}$ and $Cu_{27.5}Ge_{2.5}Te_{70}$). Furthermore, the measurements of the Seebeck coefficient as a function of temperature (Fig. 7) show an almost constant variation, particularly for the higher copper concentration samples.

The large decrease of the electrical resistivity together with low drop of the Seebeck coefficient, observed during the $Ge_{20}Te_{80}$-based conducting glasses composition optimization, lead to a huge increase of the power factor: the $Ge_{20}Te_{80}$

Table 2 Electrical transport properties of the $Ge_{20}Te_{80}$-based glasses.

Glass composition	$\rho_{300\,K}$ ($\mu\Omega m$)	$E_{a(High\ T)}$ (meV)	$S_{300\,K}$ ($\mu V/K$)	S^2/ρ ($\mu W/K^2 m$)	Reference
$Ge_{20}Te_{80}$	2.77×10^8	470	960	3.3×10^{-3}	[11]
$Cu_{15}Ge_{7.5}Te_{77.5}$	1.6×10^5	244	540	2	[14]
$Cu_{20}Ge_5Te_{75}$	2.9×10^6	263	453	1×10^{-1}	[14]
$Cu_{22.5}Ge_{2.5}Te_{75}$	6×10^3	164	415	29	[14]
$Cu_{27.5}Ge_{2.5}Te_{70}$	2.5×10^3	126	394	62	[14]
$Cu_{25}Si_5Te_{70}$	5.2×10^3	125	357	25	[15]
$Cu_{25}Ga_5Te_{70}$	2.5×10^3	134	344	47	[15]

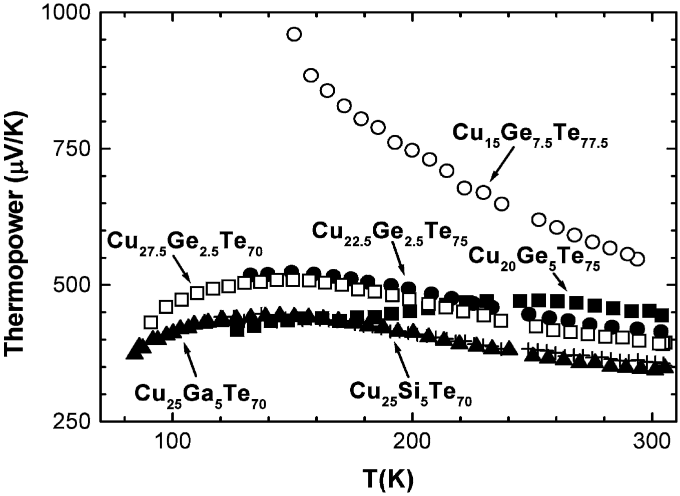

Fig. 7 Variation of the Seebeck coefficient as a function of the temperature for the $Ge_{20}Te_{80}$-based glasses.

presents a value of 3×10^{-3} $\mu W/K^2 m$, five orders of magnitude lower than the $Cu_{27.5}Ge_{2.5}Te_{70}$, which has a value higher than 6×10^1 $\mu W/K^2 m$. The very low values of thermal conductivity observed in this type of glasses (<0.2 W/Km for $Ge_{20}Te_{80}$ [14]) lead to $ZT > 0.1$ at 300 K for the $Cu_{27.5}Ge_{2.5}Te_{70}$ sample, making them interesting materials for thermoelectric applications.

The work described was only a first study of the possibility of using conducting glasses for thermoelectrical applications. Much work on the exploration of other systems and optimization of compositions is still to do, in order to get the proper materials. However, this study clearly indicates that conducting glasses are very promising materials and a strong efforts should be made to investigate their thermoelectric properties.

3.2 Bismuth Doped Tellurium Films

Low dimensional systems are actually considered one of the most important types of thermoelectric materials. Indeed, *ZT* values as high as 2.4 have already been reported in the literature for Bi_2Te_3/Sb_2Te_3 superlattice devices [16]. However, they are difficult to prepare, frequently not reproducible, and their preparation costs are very high. Therefore, the identification of new, simple and easy-to-prepare systems is also needed for these kinds of materials.

Many of the most promising recently discovered thermoelectric materials have tellurium as one of the main constituents [1]. This element has been widely studied, mainly in Japan in the late 1940s and early 1950s, for semiconductor applications, its thermoelectric properties being also explored [17–23].

Tellurium is an element that has a small value of thermal conductivity at room temperature and ambient pressure ($\sim 2\ \mathrm{W\,m^{-1}\ K^{-1}}$) [24], and presents a semiconductor behavior, with an energy gap of $\sim 340\,\mathrm{meV}$) [21, 25]. Moreover, its Seebeck coefficient was reported to be high, albeit very sensitive to impurity concentrations [22]. The electrical conductivity of pure tellurium crystals is low, but can be increased significantly with doping [22], making it a good candidate for thermoelectrical applications if higher power factor values are obtained.

Studies on tellurium low dimensional systems, in particular on films, have been performed from the beginning of the last century [17, 26–28]. However, non-reproductive behavior was observed on tellurium thin films, which was later identified as being due to the absorption of atoms and molecules at the surface [29–31]. Only for thicknesses greater than 180 nm does the effect of gas absorption become negligible [29]. Doping effect studies on tellurium films are scarce [32, 33] and, to the authors' best knowledge, no work has been made with bismuth in low dimensional systems. Moreover, only one work was recently reported on bulk materials, with the carrier concentration significantly increasing with the bismuth doping content [34]. On the other hand, several studies have been made on tellurium-doped bismuth materials [35–38]. Most probably, this discrepancy is due to the small solubility limit of bismuth on tellurium ($\sim$0.1 atom %) [34].

One way of overcoming the solubility limits imposed by thermodynamic rules can be achieved using ion implantation by introducing bismuth ions into the tellurium. Ion implantation is a well established technique in the semiconductor field and allows the incorporation of any element in a matrix to concentrations well above the equilibrium values [39]. Therefore, we decided to use the ion implantation technique to prepare films with high bismuth doping concentrations and study their effect on the electrical transport properties. Additionally, being a ballistic process, ion implantation also increases the structural disorder, with a consequent decrease of the thermal conductivity, as observed in Bi_xTe_3/Sb_2Te_3 multilayers implanted with silicon [40, 41].

The films were prepared by evaporation of high purity tellurium (99.999%, metal basis) on glass substrates and under a pressure of $<10^{-6}$ mbar, as describe elsewhere [42]. Their thicknesses were controlled during deposition in order to be insensitive to the atmospheric gases and Rutherford Backscattering Spectrometry

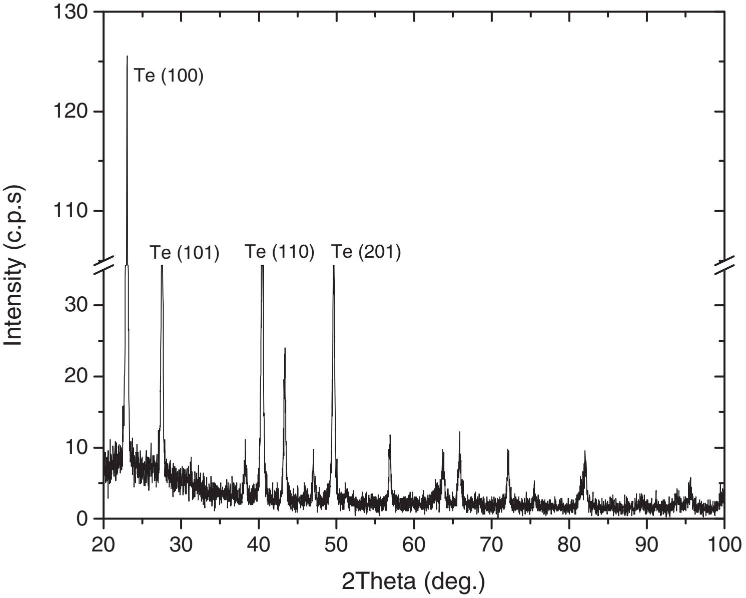

Fig. 8 Grazing incidence x-ray diffractogram of a deposited tellurium film with the major peaks labeled.

(RBS) analysis of the evaporated films confirms an average thickness of 500 nm. The quality of the films was checked by grazing incidence x-ray diffraction (GIXRD) and by scanning electron microscopy (SEM) observation, and their composition homogeneity was studied by energy dispersive x-ray spectroscopy (EDS).

Figure 8 shows a typical x-ray diffractogram of the deposited tellurium films. All peaks can be indexed to the ambient pressure tellurium trigonal crystal structure [43], albeit their intensities indicate some texture with a preferential orientation along the *a* axis.

The tellurium films were implanted with bismuth with fluences ranging from 5×10^{15} to 2×10^{16} $\mathrm{Bi}^{+}/\mathrm{cm}^{2}$. The energy was 170 keV corresponding to an implantation range of 37 nm, according the theoretical predictions of the simulation code SRIM2006 [44].

After implantation GIXRD measurements of films show no structural changes, with the diffractograms identical to the undoped ones and with all peaks belonging to the tellurium trigonal crystal structure. SEM/EDS observations of the implanted films point to a homogeneous distribution of the bismuth atoms, with no signs of visible precipitates. In any case we cannot rule out the presence of precipitates with dimensions below the detection limits of the technique. In fact the presence of pure Bi or Bi_2Te_3 precipitates in the nanometer range is a possibility to consider since the maximum concentration of Bi in the Te films highly exceeds the solubility limit.

The thickness of the implanted Te layer after the implantation and the concentration profile of the Bi were measured by RBS. The spectrum obtained for the film

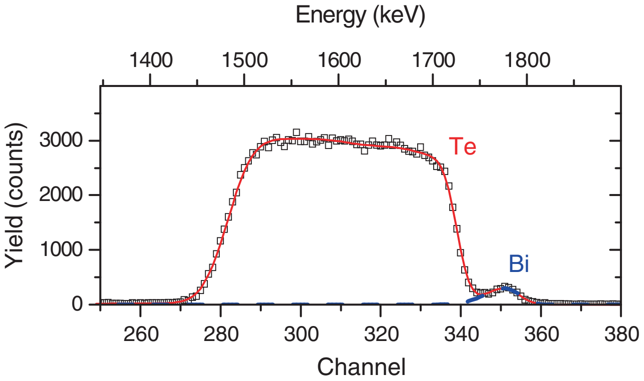

Fig. 9 Experimental RBS spectrum of a tellurium film implanted with nominally 1×10^{16} Bi^+/cm^2 implantation fluence (*open squares*) and calculated curve by assuming a Gaussian implantation profile. The measured fluence is 8.6×10^{15} Bi^+/cm^2.

implanted with $1 \times 10^{16}\,cm^{-2}$ is shown in Fig. 9. The results reveal a reduction of about 50% of the thickness of the films implanted with the highest fluences indicating that a significant sputtering effect occurred during the implantation. Also the measured fluences show a decrease of 5–10% relative to the nominal values compatible with a self-sputtering process. The Bi profile, due to the sputtering process, extends from the surface up to ~70 nm with a maximum around 20 nm (Fig. 10). The maximum concentration values measured for the implanted fluences were in the range of 3–8 atom % in the implanted regions (Fig. 10). In order to have a better control of the implantation profile further studies are necessary to establish the implantation conditions that minimize the sputtering yield. This a relevant parameter considering the low surface binding energy (2.02 eV) of Te responsible for the high sputtering yields determined.

Even though the sputtering effects limit the maximum concentration attainable of Bi in Te by ion implantation, the results clearly show that values much higher than the ~0.1 atom % reported for an equilibrium situation [34] are possible, confirming that this technique is suitable for doping tellurium with large bismuth concentrations.

The electrical transport properties of the films were studied by measuring the electrical resistivity and Seebeck coefficient variation as a function of the temperature.

A change from a semiconductor to a semimetallic behavior can be seen with the bismuth doping (Fig. 11). Annealing the implanted films at 200°C for 10 min recovers the semiconductor behavior, which is most probably due to the formation of Bi_2Te_3 precipitates. However, this point still needs further clarification. An energy gap of 56 meV (Table 3) is obtained for the unimplanted tellurium film, much lower than what would be expected for this element (~340 meV). The annealed films also show energy gaps of the same order of magnitude as the undoped sample. These

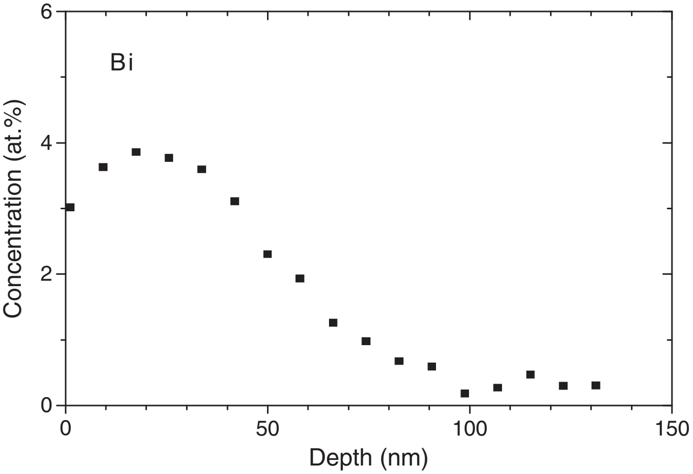

Fig. 10 Concentration profile of bismuth in a Te film implanted with a fluence of 1 × 10^{16} cm^{-2}.

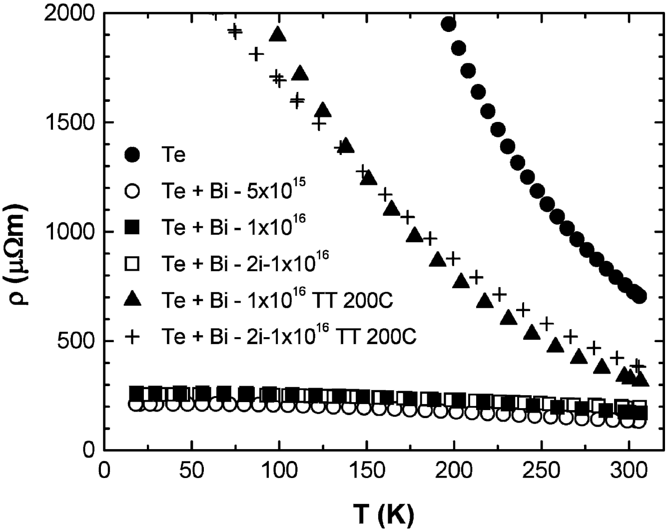

Fig. 11 Electrical resistivity of tellurium films as a function of temperature (TT 200° C represent implanted films after heat treatments at 200° C for 10 min).

lower calculated values possibly indicate that the tellurium used in the films preparation had already some impurities.

It is important to emphasize that bismuth exists only in a limited volume of the tellurium film, close to the surface and, consequently, the samples can be considered as a double layer. Therefore, a more careful analysis of the resistivity data implies the consideration of the samples as two resistances in parallel, which correspond to pure and bismuth doped tellurium regions (ρ_{Bi}). By using this approximation

Table 3 Electrical transport properties of the bismuth doped tellurium films.

Film type	$\rho_{\mathrm{Bi}300\mathrm{K}}$ ($\mu\Omega$m)	E_a (meV)	$S_{300\mathrm{K}}$ (μV/K)	S^2/ρ (μW K^{-2} m^{-1})
Pure Te	738	56	187	47
Bi impl. 5×10^{15} cm^{-2}	28	–	188	1262
Bi impl. 1×10^{16} cm^{-2}	26	–	145	809
Bi impl 2×10^{16} cm^{-2}	55	–	29	15
Bi impl. 1×10^{16} cm^{-2} HT 200°C	66	53	147	327
Bi impl 2×10^{16} cm^{-2} HT 200°C	152	50	172	194

it is possible to calculate more accurate resistivity values for the bismuth doped tellurium regions (Table 3) than the average values obtained if the total thicknesses are considered. A significant decrease of the resistivity at room temperature (of more than one order of magnitude) can be seen in the bismuth doped tellurium regions, when compared with pure tellurium. The annealing increases the resistivity values, albeit not recovering the pure tellurium ones.

Measurements of the Seebeck coefficient as a function of the temperature indicate that the conduction is mainly hole-type for all films (Fig. 12). Bismuth doping decreases the room temperature Seebeck coefficient by $\sim$25%, from $\sim 200\,\mu$V/K, for the unimplanted and 5×10^{15} cm^{-2} implanted film, to $\sim 150\mu$V/K for $1-2 \times 10^{16}$ cm^{-2} implanted films. These results are in agreement with the presence of small amounts of impurities already in the undoped films, as a Seebeck value of $-200\,\mu$V/K has been reported for high-purity bulk tellurium, together with an extreme sensitivity of thermopower to doping [22].

In all films is observed a linear decrease of the Seebeck coefficient with the decreasing temperature. Albeit they present similar values, there is a change from a convex to a concave curve with implantation, the annealing partially recovering the convex curvature, in agreement with the complex band structure of tellurium [25].

Thermoelectric power is mainly sensitive to the less electrical resistive part of the samples and, therefore, the measured Seebeck coefficients are mostly coming from those regions. In the case of tellurium films, and considering the electrical resistivity differences in the bismuth doped and undoped regions, this means that the measured Seebeck coefficients mainly come from the contribution of the bismuth doped tellurium regions, and consequently, as a first approximation, can be considered as only coming from those regions. As a result, a power factor of those regions can be roughly estimated if the calculated electrical resistivity of the bismuth doped tellurium regions and the measured Seebeck coefficients are considered.

An increase of almost two orders of magnitude in the power factor of the best doped film (bismuth implanted with 5×10^{15} cm^{-2} fluence) is observed, when compared with the pure tellurium film (Table 3). The best doped film has a power factor of $\sim 1{,}260\,\mu$W K^{-2} m^{-1}, which is already close to those obtained on the Bi_2Te_3 based phases ($2{,}000 - 4{,}000\,\mu$W K^{-2} m^{-1}) and points to a good possibility of obtaining high performance thermoelectric materials by implantation (if the thermal conductivity of bulk tellurium is considered, a ZT value of $\sim$0.2 is already obtained

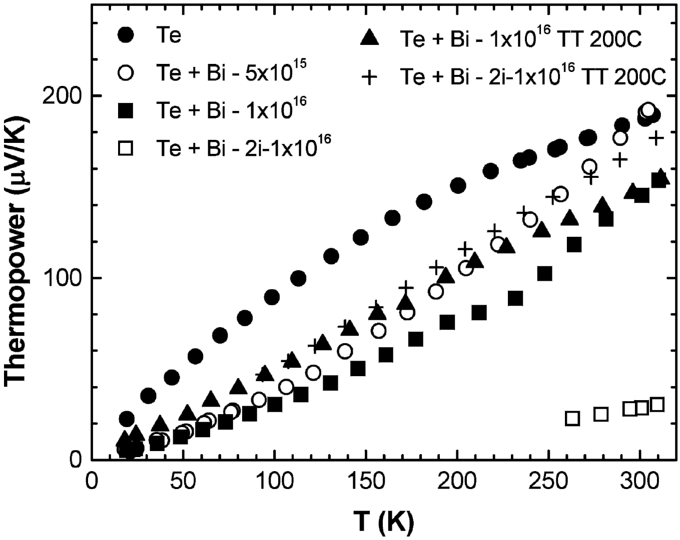

Fig. 12 Seebeck coefficients of the tellurium films, as a function of temperature (TT 200° C represent implanted films after heat treatments at 200° C for 10 min).

at 300 K for the best doped film). However, a better understanding and optimization of the implantation process is still need in order to get bismuth doped tellurium films with thermoelectric performances suitable to practical applications.

4 Conclusions

The deeper understanding of the parameters that affect the thermoelectric performance, together with the development of new concepts and the use of novel synthesis techniques, have recently led to the identification of materials with improved thermoelectric characteristics. Nevertheless, there are still strong limitations on those materials and the discovery and investigation of new systems are highly desirable.

The identification and use of general rules based on the "Phonon Glass Electron Crystal" concept, which affect the phonons propagation without changing significantly the electrical charge propagation, can lead to the development of new improved thermoelectrical systems. Here were presented two new systems, electrical conducting glasses and doped tellurium films, which we think that should be studied more deeply. Albeit not yet optimized, both show interesting thermoelectric performances, with room temperature ZT values higher than 0.1. However, much work is still to do on these two new systems, from the development of *n*- and *p*-type conducting materials and increasing of the thermoelectric performances, to the enhancement of the glass stabilization and the optimization of the implantation conditions, before they could be considered as high-efficiency thermoelectric materials with practical use. The rising of the global need for sustainable energy should encourage not only the optimization of the already identified promising systems, but also the development of new families with better thermoelectric properties.

Acknowledgments This work was partially supported by the bilateral French–Portuguese GRICES/CNRS 2007–2008 program, European COST P16 program and FCT, Portugal, under contract nr. PTDC/QUI/65369/2006. APG and CG acknowledge NATO ARW support for their participation to ARW Workshop "Properties and Applications of Thermoelectric Materials" September 20–26, 2008, Hvar, Croatia.

References

1. Godart, C., Gonçalves, A.P., Lopes, E.B. et al., this volume, 19–49.
2. Slack, G.: New materials and performance limits for thermoelectric cooling. In: Rowe D.M. (ed.) CRC Handbook of Thermoelectrics, pp. 407–440. CRC, Boca Raton, FL (1995)
3. Nagel, S.R.: Thermoelectric-power and resistivity in a metallic glass. Phys. Rev. Lett. **41**, 990–993 (1978)
4. Teoh, N., Teoh, W., Arajs, S. et al.: Absolute thermoelectric-power of amorphous metallic glass $Fe_{80}B_{20}$ between 300-K and 1000-K. Phys. Rev. B **18**, 2666–2667 (1978)
5. Carini, J.P., Basak, S., Nagel, S.R. et al.: The thermoelectric-power of the metallic glass $Ca_{0.8}Al_{0.2}$. Phys. Lett. A **81**, 525–526 (1981)
6. Pekala, K., Pekala, M., Trykozko, R.: Magnetic thermoelectric-power of $Fe_{20}Ni_{60}B_{10}Si_{10}$ metallic-glass. Solid State Commun. **46**, 413–415 (1983)
7. Bhatnagar, A.K., Prasad, B.B., Rathnam, N.R.M.: Magnetic, electric and thermoelectric studies on metallic-glass $Fe_{39}Ni_{39}Mo_4Si_6B_{12}$. J. Non-Cryst. Solids **61–2**, 1201–1206 (1984)
8. Petersen, K.E., Birkholz, U., Adler, D.: Properties of crystalline and amorphous silicon telluride. Phys. Rev. B **8**, 1453–1461 (1973)
9. Sidorov, V.A., Brazhkin, V.V., Khvostantsev, L.G. et al.: Nature of semiconductor-to-metal transition and volume properties of bulk tetrahedral amorphous GaSb and GaSb-Ge semiconductors under high pressure. Phys. Rev. Lett. **73**, 3262–3265 (1994)
10. El-Oyoun, M.A.: A study of the crystallization kinetics of $Ge_{20}Te_{80}$ chalcogenide glass. J. Phys. D: Appl. Phys. **33**, 2211–2217 (2000)
11. Parthasarathy, G., Bandyopadhyay, A.K., Asokan, S. et al.: Effect of pressure on the electrical-resistivity of bulk $Ge_{20}Te_{80}$ glass. Solid State Commun. **51**, 195–197 (1984)
12. Ferhat, A., Ollitrault-Fichet, R., Mastelaro, V. et al.: Etude des verres du système Ag-Ge-Te. J. de Physique IV **2**, C2–201-C2–206 (1992)
13. Ramesh, K., Asokan, S., Sangunni, K.S. et al.: Compositional dependence of high pressure resistivity behaviour of Cu-Ge-Te glasses. Phys. Chem. Glasses **37**, 217–220 (1996)
14. Gonçalves, A.P., Lopes, E.B., Rouleau, O. et al.: Conducting glasses as new potential thermoelectric materials: the Cu-Ge-Te case. Submitted to J. Mater. Chem.
15. Gonçalves, A.P., Lopes, E.B., Rouleau, O. et al.: to be published.
16. Venkatasubramanian, R., Siivola, E., Colpitts, T. et al.: Thin-film thermoelectric devices with high room-temperature figures of merit. Nature **413**, 597–602 (2001)
17. Fukuroi, T., Tanuma, S., Tobisawa, S.: Electric resistance, Hall effect, magneto-resistance and Seebeck effect in pure tellurium film. Sci. Rep. Res. **A1**, 365–372 (1949)
18. Fukuroi, T., Tanuma, S., Tobisawa, S.: On the electro-magnetic properties of single crystals of tellurium. I electrical resistance, Hall effect, magneto-resistance and thermo-electric power. Sci. Rep. Res. **A1**, 373–386 (1949)

19. Fukuroi, T., Tanuma, S., Tobisawa, S.: On the electro-magnetic properties of single crystals of tellurium. II Ettingshausen–Nernst effect. Sci. Rep. Res. **A2**, 233–238 (1950)
20. Fukuroi, T., Tanuma, S., Tobisawa, S.: On the electro-magnetic properties of single crystals of tellurium. III Adiabatic and isothermal Hall effect, and Ettingshausen effect. Sci. Rep. Res. **A2**, 239–248 (1950)
21. Fukuroi, T.: On the width of forbidden energy zone of tellurium. Sci. Rep. Res. **A3**, 175–181 (1951)
22. Fukuroi, T., Tanuma, S., Tobisawa, S.: Electrical properties of antimony-doped tellurium crystals. Sci. Rep. Res. **A4**, 283–297 (1952)
23. Fukuroi, T., Tanuma, S., Yoshio, M.: Electrical properties of tellurium crystals at very low temperatures. Sci. Rep. Res. **A5**, 18–29 (1953)
24. Fischer, G., White, G.K., Woods, S.B.: Thermal and electrical resistivity of tellurium at low temperatures. Phys. Rev. **106**, 480–483 (1957)
25. Deng, S., Köhler, J., Simon, A.: The flat/steep band condition created in Te-II. Physica C **460–462**, 1020–1021 (2007)
26. Warburton, F.W.: The Hall effect and resistance in sputtered tellurium films. Phys. Rev. **30**, 673–680 (1927)
27. Sakurai, T., Munesue, S.: Resistivity of evaporated tellurium films, Phys. Rev. **85**, 921–921 (1952)
28. Ghosh, S.K.: Variation of field effect mobility and Hall effect mobility with the thickness of the deposited films of tellurium. J. Phys. Chem. Solids **19**, 61–65 (1961)
29. Silbermann, R., Landwehr, G., Köhler, H.: Field effect in tellurium. Solid State Commun. **9**, 949–951 (1971)
30. Tsiulyanu, D., Tsiulyanu, A., Liess, H.-D. et al.: Characterization of tellurium-based films for NO_2 detection. Thin Solid Films **485**, 252–256 (2005)
31. Tsiulyanu, D., Stratan, I., Tsiulyanu, A. et al.: Sensing properties of tellurium based thin films to oxygen, nitrogen and water vapour. 2006 International Semiconductor Conference, Vol. **2**, pp. 287–290, Sinaia, (2006)
32. Mathur, P.C., Dawar, A.L., Taneja, O.P.: Electrical transport properties of copper-doped tellurium films. Thin Solid Films **66**, 281–285 (1980)
33. Rao, L.V., Naidu, B.S., Reddy, P.J.: Electrical-conductivity and thermopower measurements on silver doped tellurium-films. Phys. Status Solidi A **65**, K135–K138 (1981)
34. Orlov, A.M., Gonchar, L.I., Salanov, A.A.: Solubility limit and thermoelectric properties of bismuth-supersaturated tellurium. Tech. Phys. Lett. **32**, 38–41 (2006)
35. Morimoto, T.: Heavy electrons in tellurium-doped bismuth. J. Phys. Soc. Japan **21**, 1008 (1966)
36. Vangoor, J.M.N.: Hall coefficients of tellurium doped bismuth. Phys. Lett. A **25**, 442 (1967)
37. Heremans, J., Morelli, D.T., Partin, D.L. et al.: Properties of tellurium-doped epitaxial bismuth-films. Phys. Rev. B **38**, 10280–10284 (1988)
38. Red'ko, N.A., Kagan, V.D., Rodionov, N.A.: Low-temperature thermal conductivity of tellurium-doped bismuth. Phys. Solid State **47**, 416–423 (2005)
39. Ryssel, H., Ruge, I.: Ion Implantation. Wiley, New York (1986)
40. Xiao, Z., Zimmerman, R.L., Holland, L.R., et al.: MeV Si ion bombardments of thermoelectric Bi_xTe_3/Sb_2Te_3 multilayer thin films for reducing thermal conductivity. Nucl. Instr. Meth. Phys. Res. B **241**, 568–572 (2005)
41. Xiao, Z., Zimmerman, R.L., Holland, L.R., et al.: Nanoscale Bi_xTe_3/Sb_2Te_3 multilayer thin film materials for reduced thermal conductivity. Nucl. Instr. Meth. Phys. Res. B 242, 201–204 (2006)
42. Lopes, E.B., Gonçalves, A.P., Alves, E. et al.: to be published
43. Adenis, C., Langer, V., Lindqvist, O.: Reinvestigation of the structure of Tellurium. Acta Cryst. C 45, 941–942 (1989)
44. Ziegler, J.F., Biersack, J.P., Littmark, U: The Stopping and Range of Ions in Matter, Vol. 1. IBM Research, New York (2006)